

Journal of Materials Chemistry C

Accepted Manuscript



This is an *Accepted Manuscript*, which has been through the Royal Society of Chemistry peer review process and has been accepted for publication.

Accepted Manuscripts are published online shortly after acceptance, before technical editing, formatting and proof reading. Using this free service, authors can make their results available to the community, in citable form, before we publish the edited article. We will replace this *Accepted Manuscript* with the edited and formatted *Advance Article* as soon as it is available.

You can find more information about *Accepted Manuscripts* in the [Information for Authors](#).

Please note that technical editing may introduce minor changes to the text and/or graphics, which may alter content. The journal's standard [Terms & Conditions](#) and the [Ethical guidelines](#) still apply. In no event shall the Royal Society of Chemistry be held responsible for any errors or omissions in this *Accepted Manuscript* or any consequences arising from the use of any information it contains.

Size tunable elemental copper nanoparticles: extracellular synthesis by thermoanaerobic bacteria and capping molecules

Cite this: DOI: 10.1039/x0xx00000x

Received 00th January 2012,
Accepted 00th January 2012

DOI: 10.1039/x0xx00000x

www.rsc.org/

Gyoung Gug Jang^a, Christopher B. Jacobs^b, Ryan G. Gresback^b, Ilia N. Ivanov^b, Harry M. Meyer III^c, Michelle Kidder^d, Pooran C. Joshi^c, Gerald E. Jellison Jr^c, Tommy J. Phelps^a, David E. Graham^a, Ji-Won Moon^{a*}

Bimodal sized elemental copper (Cu) nanoparticles (NPs) were synthesized from inexpensive oxidized copper salts by an extracellular metal-reduction process using anaerobic *Thermoanaerobacter* sp. X513 bacteria in aqueous solution. The bacteria nucleate NPs outside of the cell, and they control the Cu²⁺ reduction rate to form uniform crystallites with an average diameter of 1.75±0.46 µm after 3-day incubation. To control the size and enhance air stability of Cu NPs, the reaction mixtures were supplemented with nitrilotriacetic acid as a chelator, and the surfactant capping agents oleic acid, oleylamine, ascorbic acid, or L-cysteine. Time-dependent UV-visible absorption measurements and XPS studies indicated well-suspended, bimodal colloidal Cu NPs (70–150 and 5–10 nm) with extended air-stability up to 300 min and stable Cu NP films surfaces with 14% oxidation after 20 days. FTIR spectroscopy suggested that these capping agents were effectively adsorbed on the NP surface providing oxidation resistance in aqueous and dry conditions. Compared to previously reported Cu NP syntheses, this biological process substantially reduced the requirement for hazardous organic solvents and chemical reducing agents, while reducing the levels of Cu oxide impurities in the product. This process was highly reproducible and scalable from 0.01 to 1-L batches.

Introduction

Elemental copper (Cu) has long been used to manufacture electronics and wiring, and more recently for the production of micro-devices, photovoltaics and biomedical devices with nanoscale forms.¹⁻⁵ Due to their unique optical, thermal, and high conductive properties, elemental Cu NPs are advantageous for designing advanced plasmonics⁴ and printable microelectronic devices^{2,3,5} compared with other noble metallic NPs, such as silver and gold. The small diameter of elemental Cu NPs confers size-dependent localized surface plasmon resonance (LSPR) features,¹ and their high surface area to volume ratio makes them attractive catalysts.⁶ However, homogeneous, oxide-free Cu NPs have been difficult to manufacture in a low-cost and scalable system because of their high reactivity and susceptibility to oxidation during synthesis and post treatments.^{2,3,5} Although syntheses using micro-emulsion, vacuum vapor deposition,¹ thermal decomposition, chemical reduction,^{2-5,7} laser ablation,⁸ bacterial⁹ and wire explosion¹⁰ methods have been reported to produce elemental Cu NPs, these methods frequently produced a mixture of Cu and Cu₂O by-products. Among these methods, wet chemical reduction is easier to control and produces relatively high yields while minimizing oxidation. Cu NPs were also reported to be cytotoxic,¹¹ therefore liquid-phase syntheses would be preferable to gas-phase syntheses for nanoparticle worker safety.

However, this synthesis requires organic solvents such as ethylene glycol, acetone, trioctylamine or toluene^{3,8,12,13,14,16} and uses hazardous reducing agents such as hypophosphites or hydrazines^{2,3,5,7,8,12,13,15,16} at high temperatures.

The bacterial synthesis of Cu NPs offers an attractive green process that minimizes hazardous reductants, reduces organic solvent usage and lowers production costs. Previous studies described the synthesis of Cu nanoparticles inside a variety of microorganisms,¹⁷ including yeast cells¹⁸ and Gram-negative bacteria⁹ that produced a mixture of Cu, Cu₂O and CuO particles. However, these biological syntheses have slower reaction rates, larger particle sizes, and significant aggregation compared to chemical synthesis in organic solvents.^{9,17,18} Moreover, many bacteria are killed by contact with copper,¹⁹ and biologically produced Cu NPs react rapidly with oxygen to produce CuO that can also be toxic.²⁰ Recently, we have achieved inexpensive, extracellular, reproducible, and scalable NP production using a biological process with thermophilic, Gram-positive bacteria growing in anoxic reaction mixtures (for example, cadmium sulfide, zinc sulfide and magnetite).²¹⁻²⁵ In this study, we prepared elemental Cu NPs using the same metal-reducing bacterium with different conditions for facilitating Cu NP nucleation and growth. This new process is readily scalable for elemental Cu NP production, because

the NPs are produced and remain outside of the bacterial cells while the anaerobic conditions minimize oxidation during synthesis. In order to control particle size and enhance stability during Cu NP purification, soluble polymers or surfactants can be added.

This study investigated 1) the synthesis mechanism of various sized biotic Cu NPs; 2) the addition of chelating agents to accelerate crystallization and/or organic/inorganic surfactants to stabilize elemental Cu NPs in aqueous solutions and films; and 3) the physical and chemical characteristics of the resulting Cu NPs.

Experimental section

Synthesis of Cu NPs. Extracellular Cu NPs were synthesized by the thermophilic metal-reducing bacterium, *Thermoanaerobacter* sp. X513.²⁴ An inoculum of mid-logarithmic growth phase cells (2 vol. %) was added to modified TOR-39 medium supplemented with 10 mM D-glucose, and the culture was incubated at 65 °C. After 1 day of cell growth to a density of approximately 2×10^8 cells/mL,²⁵ an aliquot of copper chloride was added to adjust the concentration to 2 mM CuCl₂, and then biotic Cu particles were harvested after 3 days. For crystallite growth, size confinement and stability, the chelating agent nitrilotriacetic acid (NTA) agent (0.1 wt. % of final concentration) was added at 2 days of biotic Cu particles incubation, and various surfactants including oleylamine, L-ascorbic acid, oleic acid, L-cysteine and ammonium sulfide were added after 30 min. The aqueous mixtures of oleic acid or oleylamine were added at a final concentration of 0.1 vol. % after severe shaking. The organic solvent based fatty acids and amines were prepared in a mixture of ethanol and H₂O (3:1 v/v) for scale-up. Other capping molecules were soluble in water. The effects of incubation time, surfactant dosing amounts and order of addition (e.g. *in situ* or after copper chloride addition) were evaluated to reduce particle size and increase colloidal air stability (Supplementary Information). Cu NPs were harvested by centrifugation at 8,000 rpm for 10 min and washed 4 times with N₂-purged deionized water in an anoxic glove box.

Characterization. LSPR of Cu NPs was directly measured in a transparent culture vessel using a UV-visible light spectrophotometer (HP 8453, Hewlett-Packard) during Cu NP synthesis, the enrichment of microorganisms, microbial Cu reduction phases and formation of Cu NP. The absorption spectra of redispersed Cu NP samples in water were recorded using a UV-vis spectrophotometer (Cary 100 bio, Varian) with a 1-cm tightly stoppered quartz cuvette every 10 min for 6 hrs with photographs to monitor to evaluate the colloidal stability against agglomeration and oxidation. The air-stability of the various Cu NPs in an aqueous solution was evaluated by characterizing the transition of the Cu LSPR feature to a Cu oxide excitonic feature. Fourier transform infrared (FTIR) spectroscopy measurements were carried out on the dry powders using a PIKE diamond crystal ATR on a Digilab FTS7000 FTIR spectrometer equipped with a DTGS detector, in the range of 600–4,000 cm⁻¹. An X-ray diffractometer (X'pert PRO, PANalytical, Natick, MA) equipped with Mo-K α radiation at 60 kV/45 mA from 5°–35° 2 θ was used to obtain XRD profiles. Data were analyzed by profile fitting without any structural parameters using the JADE software package (Material Data Inc.). Average crystallite size (ACS) was determined using the JADE software along with the Scherrer equation using integral breadth calculation. Surface chemistry data were obtained using X-ray photoelectron spectroscopy (XPS, K-Alpha XPS system, Thermo Fisher Scientific) equipped with a monochromated Al-K α source ($h\nu=1486.6$ eV). The 180° double focusing hemispherical analyzer with 128-channels was operated at constant pass energy of 200 eV for survey spectra and 50

eV for core level spectra. Peak fitting was performed using the Avantage program (v4.61). Spin-orbit doublets were related using the appropriate area and separation relationships after applying a Shirley background correction. Transmission electron microscopy (TEM, Libra 120, Carl Zeiss AG, Germany) and scanning electron microscopy (SEM, Merlin, Carl Zeiss AG, Germany) were used to examine the morphology and grain size of the drop casted NP film. The drop casted Cu NPs films were prepared by re-dispersing in methanol forming a paste with a concentration of 20–30 wt. %. The paste was deposited on carbon tape attached to glass slides or a micro platinum finger electrode and dried in a glove box. Current (I)-Voltage (V) curves were measured by a high-current source meter using a 2-point probe configuration (Keithley 2420), and the resistivity of the copper film was calculated using the dimension of electrodes (thickness= 90/10 (Pt/Ti) nm, length=2.14 mm, width=20 μ m, inter finger distance=20 μ m). To remove surfactants and organic matters, the copper films was annealed from 200 to 500 °C under an Ar atmosphere.

Results and discussion

Characterization of biosynthesized copper nanoparticles with capping molecules. Bacterial synthesis produced elemental copper particles with well-defined size distributions, confirmed by XRD, SEM, and TEM analyses (Table 1). We also found that addition of CuCl₂ to uninoculated TOR-39 medium with glucose produced Cu crystallites with a bimodal size distribution at 65 °C after a 2-day incubation period. The large, micron-sized Cu crystallites from both the biotic (BCu) and abiotic (AbCu) syntheses had similar sizes, (Fig. 1a and inset). For AbCu formation, reducing glucose molecules transfer an electron from their hemiacetal group to complexed Cu²⁺, producing red copper oxide precipitates in hot alkaline solutions (Fehling's test). In the absence of alkali or ligands, disproportionation of the Cu⁺ could produce elemental Cu. Abiotic mineralization of Cu was achieved at 65 °C but not observed below 65 °C (*i.e.* 4, 20 or 37 °C) or in solutions without glucose. The addition of nitrilotriacetic acid (NTA) chelating agent or surfactant to the abiotic system constantly produced micron-sized NPs without reducing nanometer dimensions. (Fig. S1). However, the addition of NTA to the biotic synthesis at 2 days Cu incubation (CuN), as shown in Fig. 1b, led to the formation of spherical shaped particles with reduced size and a bimodal distribution. The small particles were identified by TEM (Inset Fig. 1b). The harvested BCu contained elemental Cu while AbCu and CuN were mixtures of Cu and Cu₂O (Table 1).

After NTA addition, various capping agents were introduced to stabilize the colloidal NPs, including oleic acid (CuNO), L-cysteine (CuNC), ascorbic acid (CuNA), and oleylamine (CuNM). The CuNO NPs had a bimodal distribution that was similar to CuN, while addition of the other capping agents increased their bimodal particle sizes and formed various shaped elemental Cu crystallites (Table 1 & Fig. 1). SEM images of CuNO and CuNM particles were not obtained due to an insulating surface charging effect that was caused by nonconductive shells of oleic acid and oleylamine. The biotic CuNO NPs were smaller than abiotic Cu NPs previously synthesized by chemical reaction with addition of oleic acid at 150 °C, which had a bimodal distribution averaging 108.3 and 42.3 nm diameters.¹²

Extracellular biosynthesis of air-stable nanoparticle. The bacteria act as both reducing agents and additional nucleation sites for Cu formation. The cells enzymatically oxidize glucose and transfer electrons to transition metal ions near their cell surfaces resulting in

the reduction of the Cu^{2+} as an electron acceptor.^{21–23} However, electrons can also be transferred directly from glucose to Cu^{2+} in an exergonic reaction.²⁶ To identify factors that control crystallite growth and reduce surface oxidation, cheletor and capping molecules were added to the bacterial nanoparticle syntheses. Oleic acid-capped Cu NPs formed on the outside of the filamentous cells with 70–100 nm diameters and characteristic surface charging (Fig. 2). In contrast, surface-conductive micron-sized BCu crystallites, as shown in the inset, detached from the cell surfaces and continued the chemical crystal growth.

The addition of CuCl_2 changed the white microbial enriched media to a typical blue color (Inset Fig. 3a-1), which exhibited a monotonic decline in absorption from the blue to red wavelengths (Fig. 3b-1). After 2 days incubation, the blue color thinned and brown aggregates precipitated via microbial reduction, and Cu crystal nucleation appeared to start in the media. During an additional 1–3 days incubation, the solution changed to a yellow color and brown-red BCu particles with micron size precipitated after 3 days incubation (Fig. 3a-2 & Inset). The control of incubation time between 2 and 3 days showed no crystal size confinement to less than 100 nm (Fig. S2) and the uncapped Cu easily oxidized in an hour. Fig. 3b-2 shows that an absorption peak arose at 570 nm compared with the featureless spectra of the CuCl_2 precursor solution (Fig. 3b-1). This peak can be assigned to a characteristic Cu LSPR feature that appears around 550–600 nm, depending on the existence of oxide layer and the size of the Cu NPs. Large (20–30 nm) and small (<10 nm) diameter Cu NPs have features at 587 nm and 578 nm, respectively.⁷ TEM image analysis showed that BCu crystallites also have a small portion of NPs with 20 nm diameter (not shown). The LSPR peak at 570 nm may be attributed to the small BCu NPs.

The growth of Cu NPs was facilitated by an addition of NTA as a chelating agent at 2 days incubation. After NTA addition for 30 min, the yellow-blue solution containing remaining Cu^{2+} gradually turned red and then changed to burgundy color (Inset Fig. 3a-3). For CuN, *in situ* absorption spectra showed that a noticeable LSPR of facilitated biotic Cu NPs arose at 590 nm (Fig. 3b-3). The XRD patterns of CuN and AbCu (Fig. 3a-4) exhibited elemental Cu and Cu_2O peaks due to surface oxidation during the post harvesting procedure and XRD measurement in air. The average crystal size (ACS) of CuN was 50 nm. Oleic acid capped CuN (CuNO) showed oxide free Cu with 75 nm of ACS (Fig. 3a-5). Another abiotic control experiment tested the effects of NTA on AbCu particle formation after incubation times of 0, 1 and 2 days. The addition of NTA resulted in no Cu reduction at 0 day and micron-size Cu crystals at 1 and 2 days (Table. S1). Compared to the formation rate of BCu NP, the abiotic kinetics of Cu^{2+} reduction are relatively fast, resulting in micron-size crystallites.

The re-dispersed BCu NPs (inset of Fig. 3b-2') in water exhibited clear LSPR characteristics at 605 nm due to aggregation. Therefore the spectra of BCu or AbCu were obtained immediately after severe shaking. Inset Fig. 3b-3' shows the re-dispersed CuN NPs exhibited a LSPR peak at 587 nm, which is blue-shifted compared with the re-dispersed BCu NPs. The LSPR maxima at 587 nm correspond to 50–70 nm diameter Cu NPs in an aqueous solution.²⁷ The optical responses matched TEM, SEM, and XRD measurements. For AbCu, the absorption spectra exhibited a featureless band between 400 and 800 nm (Fig. 3b-4) due to fast precipitation and large particle sizes. The re-dispersed AbCu NPs (Fig. 3b-4') exhibited a LSPR peak at 606 nm similar to BCu NPs. Sub-micron size AbCu NPs with <500 nm diameter may contribute to the LSPR feature.

Effect of capping molecules on suspended solution. The addition of capping agents improved NP stability in aqueous solution to 3–15 times longer than CuN by protecting against oxidation and colloidal agglomeration. Time course photographs in Fig. 4a show changes in the color and colloidal behavior of various Cu NPs in aqueous solution during air exposure. The suspensions were sealed until spectral measurement in an open-air environment. The colloidal CuNO NPs suspended well for 180 min and gradually precipitated after 240 min during air exposure (Fig. 4a-B). The solution's red color gradually darkened through 180 min and precipitated at 360 min. However, the color of CuN NPs darkened around 30 min and turned to white green with precipitation at 180 min. Fig. 4b & c show the corresponding UV-vis absorption spectra and LSPR feature corresponding to capping molecules and reaction time, respectively. The corresponding UV-vis absorption spectra of CuNO after air exposure indicated that the LSPR peak at 580 nm at 0 min redshifted to 590 nm over 240 min, while the LSPR peak of CuN shifted from 587 nm to 598 nm in 60 min and then disappeared (Fig. 4c). The oxidation of colloidal Cu NPs that appear red (due to a LSPR feature at 560–610 nm) produces colloidal amorphous and/or crystallite Cu_2O NPs that appear green due to an excitonic feature at 720–750 nm corresponding to its band gap.¹⁴ Also, the particle size determining peak position and intensity, the presence of a copper oxide layer,^{4,14} the degree of agglomeration of particles,¹⁵ and a combination above affect the LSPR features of the suspended Cu NPs.²⁸ Another study showed that 8 nm CuO NPs exhibit an absorption peak at 630 nm.¹⁶ Increasing the aggregate sizes of colloidal Cu NPs leads to red-shifting of the Cu LSPR and finally quenching the plasmonic feature of the nano-size regime via agglomeration, similar to bulk-phase copper.¹⁵ The surface coating formed by the long carbon chains of oleic acid effectively maintained colloidal NPs in suspension.

Depending on capping agents (Fig. 4b), colloidal Cu NPs exhibited tunable LSPR peaks from 580 nm to 600 nm due to different size and refractive index induced by the different adsorbed organic layers. The addition of ascorbic acid stabilized CuNA NPs for the longest period against oxidation and agglomeration (Fig. 4c & Table 1), because ascorbic acid is both an antioxidant and a capping agent. CuNA had a bimodal particle distribution. During the initial 10 min, large particles (147 nm) appeared to be quickly agglomerated and precipitated. However, small particles (10 nm) were well dispersed and slowly precipitated over 300 min.

Larger micron-size particles of AbCu and BCu (Fig. 4a-F & G) easily precipitated within 10 min. Also, the LSPR peak position and relative LSPR peak intensity were quickly quenched in one hour due to fast precipitation. The characterization of ammonium sulfide, an inorganic surfactant, was excluded because of the unavoidable formation of copper sulfide NPs. It was reported that a capped abiotic Cu NP dispersion in organic solvent was stable for several weeks in a closed system.¹³ Also, storing as-synthesized Cu NP in inorganic solution was stable for several days.²⁴ However, abiotic Cu NPs prepared in an oxidative environment were unstable and were completely precipitated after a few hours.^{6,14,29}

Structure of capping molecules on nanoparticles. To confirm the adsorption of capping molecules on the surface of Cu NPs, FTIR measurements were performed with reference spectra of BCu (Fig. 5a). The bacteria produce ethanol, acetate and lactate from glucose as major fermentation products, as well as macromolecules including proteins containing amine and carboxylic acid groups.^{25,30} For example, ZnS NPs produced by these bacteria contained organic matter, as indicated by $\nu(\text{CH}_2)$ and $\nu(\text{CH}_3)$ group vibrations.²⁵ The short-chain organic acids may have adsorbed on the Cu NP surface

and prevented oxidation, partially explaining the lower surface oxidation of BCu compared to AbCu. These peaks were not clearly noticeable on BCu due to the relatively small fraction of organic matter bound to the surface of micron-size particles. CuN exhibited absorption bands characteristic of CH₂ and CH₃ around 2920–2960 cm⁻¹ and asymmetric and symmetric vibration bands of deprotonated carboxylic acid group at 1625 cm⁻¹ and 1386 cm⁻¹ which were contributed by surface-bound NTA.^{31,32} The vibration bands at 1530 cm⁻¹ and 1440 cm⁻¹ were assigned to asymmetric and symmetric C=O stretchings of the carboxylate group,³² which may be contributed by NTA or other organic matter. For CuNO, absorption bands of the CH₂ and CH₃ groups clearly emerged due to the long carbon chain of oleic acid and a new bending mode of C=O at 1710 cm⁻¹ emerged due to oleic acid adsorbed on the Cu surface as a bilayer. The bilayer of oleic acid on CuNP was confirmed by thermogravimetric analysis, which exhibited two distinct mass loss phases at 230 °C and 425 °C (not shown).³³ Characteristic FTIR features of other capped Cu NPs are available in supplementary information.

Anti-oxidative effect of capping molecules on films. In a colloidal suspension, the entire NP surface may be exposed to dissolved oxygen diffusion, while in NP films only the top surface of aggregated particles may be directly exposed to air. The aggregation with capping molecules forms tortuous paths inside the film that significantly retard air diffusion. The kinetics of surface oxidation in an aggregated NP film are different from a colloidal suspension. Therefore time-dependent monitoring is necessary to characterize the resistance to oxidation in a dry NP film. In the XPS spectra of Cu2p_{3/2}, the peaks at 932.1, 932.6 and 934.6 are assigned to Cu, Cu₂O, and CuO, respectively.^{2,3} CuO is a thermodynamically stable phase in air; however, the Cu₂O phase can be stable when the particle size is smaller than 25 nm.^{2,16}

Based on the time course semiquantitative analysis, the atomic fraction of the surface oxide layer of Cu NPs was influenced by capping agents. Fig. 5 a&b and Table 1 show the fraction of Cu NPs surface oxide formation over 20 days. The CuO peak was assigned based on its position and satellite peaks at 940–950 eV.³ The BCu surface oxidized less rapidly than an AbCu surface. CuNO exhibited the lowest amount of surface oxide formation for 20 days. The longer chain lengths and additional hydroxyl groups were densely packed on the Cu surface, which restricted oxygen diffusion to the metal during air exposure, resulting in reduced surface oxide and thus a thinner oxide layer. Other capped NPs exhibited large Cu2p_{3/2} peak broadening due to a few nanosized clusters and surface oxidation layer formation of Cu₂O and CuO (e.g. shell-skin).³⁴ The oxidation amount was determined by deconvolution of Cu₂O, CuO and Cu peaks (Table 1). It appears that the surface oxide layer of all capped Cu NPs was formed within 5 days, and the oxide layer and capping molecules prevented further oxidation through passivation. Abiotic Cu NPs capped with oleic acid also showed a similar stabilization process resulting in formation of an oxidation layer at day 0 and stabilized with 0.2 fractions during 5 days.²

Scalable nanoparticle production and electrical properties. The scalability of bacterial elemental Cu NP production was tested by increasing the medium volume 100-fold using a 1000 mL medium volume with the same dosing ratio of glucose, Cu and capping molecules. Yields of four capped Cu NPs such as CuNO, CuNA, CuNM and CuNC NPs were 0.176 g/L, 0.154g/L, 0.198 g/L and 0.088 g/L, respectively. Scaling showed no significant influence on the morphological (SEM), crystalline structural (XRD), chemical structural (XPS, FTIR) properties of colloidal Cu NPs. (Figs. S5 and S6)

The electrical properties of Cu NPs were further studied using CuNO NP pastes, which were re-dispersed in ethanol with a particle content of 30 wt. %. CuNO was selected due to its high air stability in colloids and its low surface oxidation. Fig. 5d shows the I-V curves of the annealed Cu NP films exhibiting an increased current response to increased temperature at 200, 300, 400 and 500 °C. The black square dot line represents a reference Pt film curve in our system (the resistivity of bulk Pt is 10.6 μΩ·cm). Considering the dimensions of the electrode and reference, the calculated resistivity values were 5.25×10⁹, 1.36×10³, 147 and 652 μΩ·cm, respectively. The resistivity of abiotic Cu NPs was reported between 11 and 92 μΩ·cm.^{2,3} Inset Fig. 5d showed the corresponding SEM images of annealed CuNO at 300 °C. At high temperature, capping molecules and biomaterials started to decompose, and densification of neighbors with removal of capping molecules was observed at 300 °C. The high resistance suggests that annealing at 300 °C may partially remove capping molecules and fermentative organics and form surface oxidation through exposed surfaces. At 400 °C, the electrical property was improved, but further annealing did not reduce the resistivity. Organic fermentation products and excess capping molecules bound tightly to the NP surfaces resulting in high resistivity. Thus, new methods for NP harvesting and washing with organic solvents and detergents are of particular interest in follow-on work. Also, future optimization of the ratio of chelator and capping molecules is expected to reduce the excessive amount of organic matter contamination and improve electrical properties.

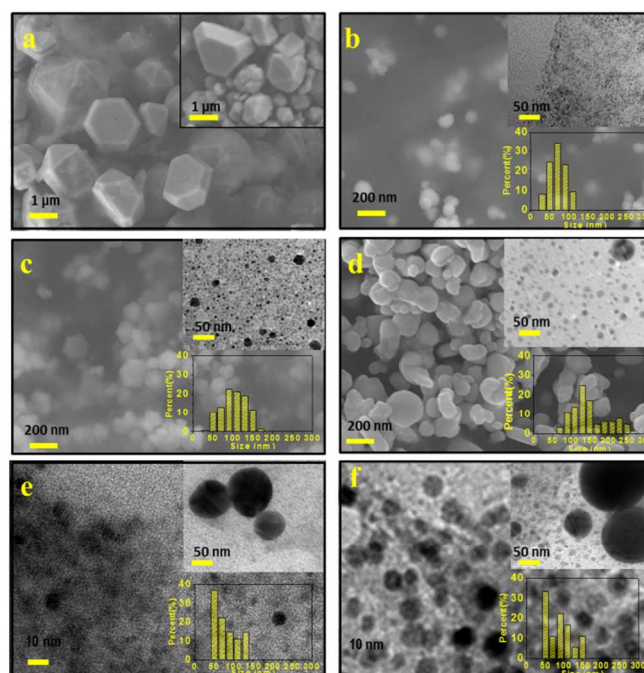


Fig. 1 TEM and SEM images of synthesized Cu NPs and corresponding size distributions for small particles (upper right inset) and large particles (lower right inset) (a) Biotic Cu crystallites (BCu) with abiotic Cu crystallites inset (AbCu); (b–f) Biotic Cu NPs formed in the presence of NTA with surfactants as follows: (b) without surfactant (CuN), (c) post treated with L-cysteine (CuNC), (d) addition of ascorbic acid (CuNA), (e) addition of oleic acid (CuNO), (f) addition of oleylamine (CuNM). The smaller particles from the bimodal distribution were observed using TEM (Inset (b), (c), (d) and main (e), (f)).

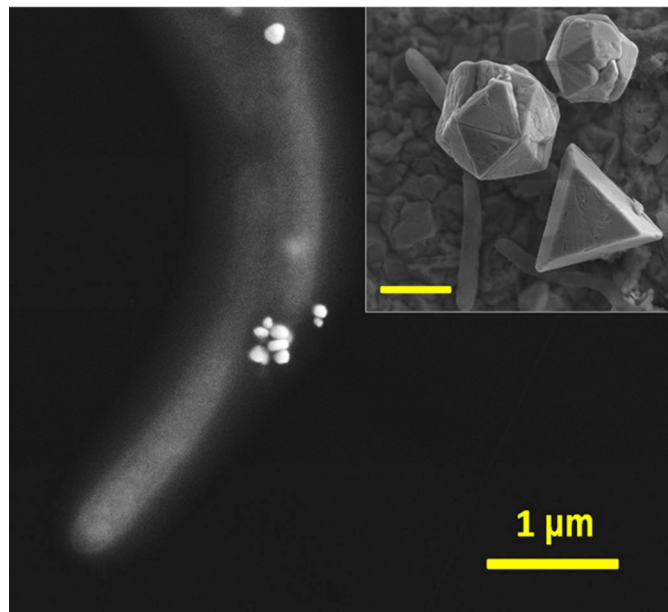


Fig. 2 SEM image of bacteria and oleic acid capped Cu nanoparticle (CuNO) in the bacterial medium. The inset shows BCu crystallites formed near bacteria. The scale bars represent 1 μm .

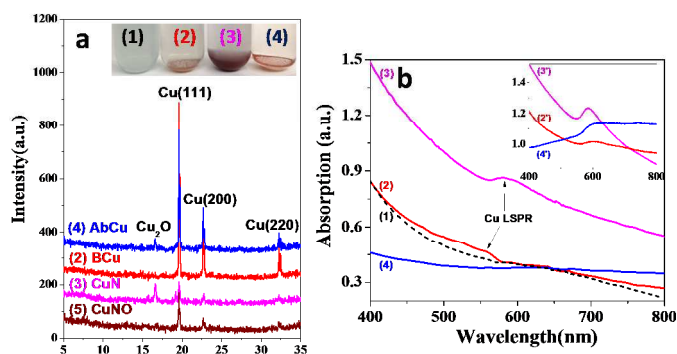


Fig. 3 (a) XRD patterns for powders separated from the Cu reaction medium. Inset is a photograph of Cu NPs forming in situ: (1) CuCl_2 precursor solution, (2) Bacteria incubated with CuCl_2 for 3 days [BCu], (3) Bacteria incubated with CuCl_2 with NTA added after 2 days incubation [CuN], (4) Abiotic CuCl_2 incubation for 2 days [AbCu], (5) Oleic acid capped CuN (b) Corresponding UV-vis absorption spectra for each anoxic mixture from part a *in situ*. Inset is spectra of re-dispersed Cu NPs in aqueous solution: (2') BCu, (3') CuN and (4') AbCu. Arrows indicate the Cu localized surface plasmon resonance (LSPR) feature of Cu NPs.

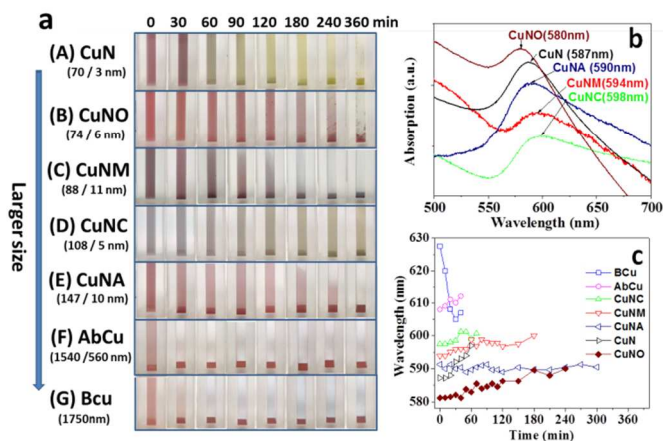


Fig. 4 (a) Time-course photographs illustrate the changes in color and precipitation of colloidal Cu NPs during air exposure. The brackets represent NPs size from microscopic image analysis (b) Optical absorbance spectra of the colloidal Cu NPs shown in Fig. 3 at 0 min. (c) Corresponding spectra of CuN NPs changed as the NPs oxidized (spectra were measured every 10 min for 120 min and every 30 min after 120 min).

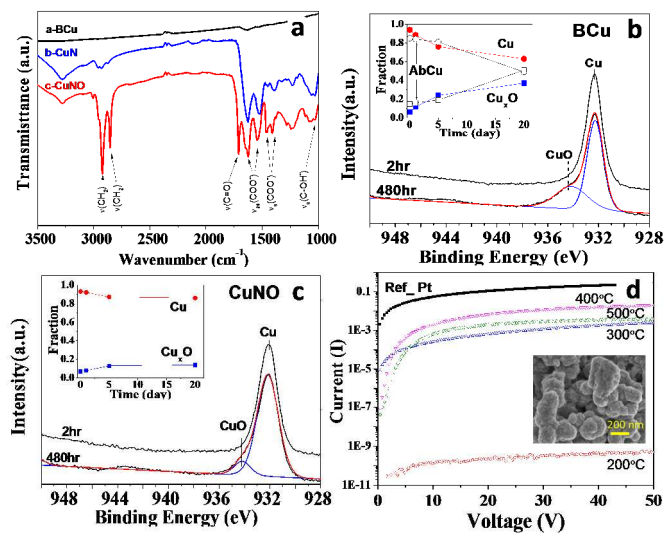


Fig. 5 (a) FTIR spectra of the indicated Cu NPs. The spectra are offset to show the vibration bands characteristic of adsorbed organic coatings. Time course XPS Cu 2p spectra of Cu NP films for 20 days: (b) BCu and (c) CuNO. Inset are XPS based semiquantitative analyses of drop casted Cu NP films exposed for the indicated number of days in ambient air. The Cu fraction is shown with circle symbols, while square symbols show the oxyc phase fraction, Cu_xO , including both CuO and Cu_2O . The inset in part A compares biotic Cu NPs (filled symbols) with abiotic Cu NPs (open symbols) (d) I-V curves of CuNO NPs films with increasing annealing temperature from 200 $^\circ\text{C}$ to 500 $^\circ\text{C}$. Inset is an SEM image of CuNO at 300 $^\circ\text{C}$.

Table 1. Description and characteristics of Cu NPs

Cu NPs	Additive	XRD (as-syn.)	Size (TEM&SEM)	Cu LSPR (nm)	Colloidal /Oxidation stability (min)	XPS Oxidation fraction		
						1	5	20 day
AbCu	None (Abiotic)	Cu ⁰ + Cu ₂ O	1.54±0.34 μm (n=18) /0.56±0.17 μm(n=21)	608	20/(>360) ^a	0.16	0.19	0.51
BCu	None (Biotic)	Cu ⁰	1.75±0.46 μm (n=20)	628	40/(>360)	0.06	0.24	0.38
CuN	NTA	Cu ⁰ + Cu ₂ O	70.1 ±21.3 nm (n=147) /2.7 ±0.8 nm (n=420)	583	300/60	0.15	0.29	0.37
CuNA	NTA + Ascorbate	Cu ⁰	147.2±49.2 nm (n=63) / 9.8±4.1 nm (n=363)	590	300/(>360)	0.26	0.29	0.34
CuNO	NTA + oleic acid	Cu ⁰	74.6±30.6 nm (n=21) / 5.6±1.2 nm (n=82)	580	270/(>360)	0.08	0.13	0.14
CuNC	NTA + cysteine	Cu ⁰	107.6 ±31.5 nm (n=146) / 5.2 ±2.0 nm (n=1092)	598	360/70	0.12	0.18	0.20
CuNM	NTA + oleylamine	Cu ⁰	87.9±40.6 nm (n=18) /11.1±2.5 nm (n=48)	594	150/(>360)	0.20	0.24	0.25

* XRD was measured to as-synthesized samples.

*(>360) of oxidation stability : Red shift of LSPR position was less than 10 nm for 360 min, but the peak shift could not be measured due to precipitation via aggregation.

*Time course oxidation fraction change was determined by an initial FWHM of Cu_{2p_{3/2}} spectra peak at 0 days, as a reference.

Conclusions

Elemental copper nanoparticles with a bimodal distribution of 70 and 3 nm diameters were biosynthesized using bacteria with the *in situ* addition of chelating and capping agents. This method substantially enhanced air stability and resistance to oxidation of colloidal NP in aqueous solution and thin films, demonstrated by examination of the Cu LSPR feature and XPS measurements. FTIR spectra indicated that chelating and capping agents coated the NP surfaces despite heterogeneous bacterial organic matter produced during the microbial activity. These coatings protected the surface from air oxidation in aqueous and dry film conditions. The chelating agent, NTA, effectively facilitated the growth of particle and limited the size to 70 nm. Fatty acids and amines capped Cu NPs without causing an increase in size, stabilized them against oxidation and agglomeration in aqueous solution and enabled the formation of the most stable elemental Cu NP film.

Acknowledgements

The authors gratefully acknowledge the support of the US Department of Energy (DOE), Advanced Manufacturing Office, Low Temperature Material Synthesis Program (CPS 24762) and of the Oak Ridge National Laboratory (ORNL). Part of this research was conducted at the Center for Nanophase Materials Sciences, which is sponsored by the ORNL Scientific User Facilities Division and DOE Office of Basic Research Sciences. FTIR work provided by M. K. K. was supported by the US DOE, Office of Science, Basic Energy Sciences under Award ERKCC96. We appreciate helpful comments about NP properties from Beth Armstrong. ORNL is managed by UT-Battelle, LLC, for DOE under contract DE-AC05-00OR22725. The U.S. Government is authorized to reproduce and distribute reprints for Government purposes notwithstanding any copyright notation hereon. G-G.J. performed synthesis experiments, analyzed data, and prepared text for the manuscript. C.B.J., R.G.G. and I.N.I. carried out SEM, TEM, TGA and other imaging experiments. H.M.M. assisted in XPS and analysis of its results. M.K. performed FTIR and its analysis. P.C.J. and G.E.J. assisted in

developing electrical analysis apparatus and methods and reviewing electrical analysis. T.J.P. provided constructive guidance and comments about the manuscript. D.E.G. and J.M. directed the work, organized its presentation and finalized the text.

Notes

^a Biosciences Division, Oak Ridge National Laboratory (ORNL), Oak Ridge, TN 37831

^b Center for Nanophase Materials Sciences Division, ORNL, Oak Ridge, TN, 37831

^c Materials Science and Technology Division, ORNL, Oak Ridge, TN 37831

^d Chemical Science Division, ORNL, Oak Ridge, TN 37831

Electronic Supplementary Information (ESI) available: [details of any supplementary information available should be included here]. See DOI: 10.1039/b000000x/

References

- G.H. Chan, J. Zhao, E.M. Hick, G.C. Schatz and R.P. Van Duyne, *Nano. Lett.*, 2007, **7**, 1947-1952.
- S. Jeong, H. Song, W. Lee, S. Lee, Y. Choi, W. Son, E. Kim, C. Paik, S. Oh and B. Ryu, *Langmuir*, 2011, **27**, 3144.
- S. Jeong, K. Woo, D. Kim, S. Lim, J. Kim, H. Shin, Y. Xia and J. Moon, *Adv. Funct. Mater.*, 2008, **18**, 679.
- M. Souza, P. Corio and A. Brolo, *Phys. Chem. Chem. Phys.*, 2012, **14**, 15722.
- D. Deng, Y. Jin, Y. Cheng, T. Qi and F. Xiao, *ACS Appl. Mater. Interfaces*, 2013, **5**, 3839.
- C.W. Li, J. Ciston, M.W. Kanan, *Nature*, 2014, **508**, 504.
- D. Deng, Y. Cheng, Y. Jin, T. Qi and F. Xiao, *J. Mater. Chem.*, 2012, **22**, 23989.
- R. Tilaki, A. Iragizad and S. Mahdavi, *Appl. Phys. A*, 2007, **88**, 415.
- S. Hasan, S. Singh, R. Parikh, M. Dharne, M. Patole, B. Prasad and Y. Shouche, *J. Nanosci. Nanotechnol.*, 2008, **8**, 3191.
- Y. Lee, B. Bora, S. Yap and C. Wong, *Curr. Appl. Phys.*, 2012, **12**, 199.

- 11 Song, L., M. Connolly, M. L. Fernández-Cruz, M. G. Vijver, M. Fernández, E. Conde, G. R. de Snoo, W. J. G. M. Peijnenburg, J. M. Navas, *Nanotoxicology*, 2014, **8**, 383.
- 12 S. Jeong, S. Lee, Y. Jo, S. Lee, Y. Seo, B. Ahn, G. Kim, G. Jang, J. Park, B. Ryu and Y. Choi, *J. Mater. Chem. C*, 2013, **1**, 2704
- 13 Y. Lee, J. Choi, K. Lee, N. Stott and D. Kim, *Nanotechnology*, 2008, **19**, 415604.
- 14 K. Rice, E. Walker, M. Stoykovich and A. Saunders, *J. Phys. Chem. C*, 2011, **115**, 1793.
- 15 S. Ghosh, D. Rahman, A. Ali, A. Kalita, *Plasmonics*, 2013, **8**, 1457.
- 16 M. Yin, C. Wu, Y. Lou, C. Burda, J. Koberstein, Y. Zhu and S. O'Brien, *J. Am. Chem. Soc.*, 2005, **127**, 9506.
- 17 G Shobha, M. Vinutha, S. Ananda, *Inter. J. Pharm. Sci. Inv.*, 2014, **3**, 28.
- 18 M. R. Salvadori, R. A. Ando, C. A. Oller do Nascimento, B. Corrêa. *PLOS ONE*, 2014, **9**, e87968.
- 19 S. Mathews, M. Hans, F. Mücklich, M. Solioz., *Appl. Environ. Microbiol.* 2013, **79**, 2605.
- 20 Y. Abboud, T. Saffaj, A. Chagraoui, A. El Bouari, K. Brouzi, O. Tanane, B. Ihssane, *Appl. Nanosci.*, 2013, **4**, 571.
- 21 J. Moon, I. Ivanov, C. Duty, L. Love, A. Rondinone, W. Wang, Y. Li, A. Madden, J. Mosher, Z. Hu, A. Suresh, C. Rawn, H. Jung, R. Lauf and T. Phelps, *J. Ind. Microbiol. Biotechnol.*, 2013, **40**, 126
- 22 J. Moon, C. Rawn, A. Rondinone, L. Love, Y. Roh, S. Everett, R. Lauf, T. Phelps, *J. Ind. Microbiol. Biotechnol.*, 2010, **37**, 1
- 23 Y. Roh, R. Lauf, A. McMillan, C. Zhang, C. Rawn, J. Bai and T. Phelps, *Solid State Communication*, 2001, **118**, 529.
- 24 Y. Roh, S. Liu, G. Li, H. Huang, T. Phelps and J. Zhou, *Appl. Environ. Microbiol.*, 2002, **68(12)**, 6013.
- 25 J. Moon, I. Ivanov, P. Joshi, B. Armstrong, W. Wang, H. Jung, A. Rondinone, G. Jellison, H. Meyer, G. Jang, R. Meisner, C. Duty and T. Phelps, *Acta Biomater.* 2014, **10**, 4474.
- 26 U.S. Shenoy, A. N. Shetty, *Appl. Nanosci.* 2014, **4**, 47
- 27 M. Usman, N. Ibrahim, K. Shameli and N. Zainuddin, *Molecules*, 2012, **17**, 14928.
- 28 V. Grassian, *J. Phys. Chem. C*, 2008, **112**, 18303.
- 29 T.M. Dang, T.T.T. Le, E. Fribourg-Blanc, M.C. Dang, *Adv. Nat. Sci.: Nanotechnol.*, 2011, **2**, 015009.
- 30 Q. He, P. Lokken, S. Chen, J. Zhou, *Biores. Tech.*, 2009, **100**, 5955.
- 31 P. Rigler, W. Ulrich, P. Hoffmann, M. Mayer, H. Vogel, *Chemphyschem*, 2003, **4**, 268.
- 32 B. Tural, M. Kaya, N. Ozkan, M. Volkan, *J. Nanosci. Nanotechnol.*, 2008, **8**, 695.
- 33 Q. Lan, C. Liua, F. Yang, S. Liu, J. Xu, D. Sun, *J Colloids Interfaces Sci.* 2007, **310**, 260.
- 34 Y. Sohn, D. Pradhan, L. Zhao, K.T. Leung, E, *Electrochemical and Solid-States Letters*, 2012, **15(4)**, K35

TOC. Elemental Cu nanoparticles in aqueous solution were synthesized by a biological process using anaerobic, metal-reducing bacteria, chelator and capping molecules

